

Computational Algebra Project: Maps, Sets and Fractals

Daniel Slocombe, Srikrishna Subrahmanyam
Tom Grigg, Vaibhav Krishnakumar

March 2015

Contents

| | |
|-----------------------------------|----------|
| 1 Maps | 1 |
| 1.1 Methods | 1 |
| 1.2 Verhulst Process | 2 |
| 1.3 Logistic Map | 4 |
| 1.4 Trigonometric Map | 5 |
| 1.5 Feigenbaum Constant | 6 |
| 1.6 Final Observations | 6 |
| 2 Sets and Fractals | 7 |
| 2.1 Definitions | 7 |
| 2.2 Mandelbrot Set | 9 |
| 2.2.1 Plots | 10 |
| 2.3 Julia Sets | 13 |
| 2.4 Compact Sets | 14 |
| 2.5 Boll's results | 14 |

1 Maps

This section focuses on our investigations of three non-linear real maps: the Verhulst process, the logistic map and the trigonometric map. Our primary aim in each investigation was to analyse the convergence to any fixed/periodic points as well as the dynamics of these points as we vary each map's parameters (namely, r and x_0). For each map, we initially approached the investigation mathematically to gather as much understanding as possible before the calculations became too tedious at which point we switched to a numerical approach. A common feature to all three maps is the occurrence of a period doubling cascade, which is a sequential doubling of the period of the iterates under a given function. This characteristic necessitates the introduction of the concepts below.

1.1 Methods

An n -periodic point under an iterative function f is a point which is invariant after n applications of f :

$$x_k = x_{k+n}$$

A point is referred to as a *fixed point* if it is a 1-periodic point:

$$x_k = x_{k+1}$$

In general, when looking for bifurcations of increasing period using purely mathematical methods, it is easy to form the equation we need to solve to ascertain any points of interest. However, solving these equations typically becomes increasingly difficult with the period of the points we're looking for.

For small periods however, we can find an n -periodic point by simply applying the iterative function n -times and supposing equality with the initial value:

$$x_k = x_{k+n} = f(x_{k+(n-1)}) = f^n(x_k) \quad (*)$$

A fixed point is either attractive or repulsive and the distinction is important when considering the iterative behaviour of points in its vicinity.

An **attractor** is a fixed point to which the argument of an iterative function will tend to. However, if the iterates move away from this point then it is referred to as a **repeller**.

There is a simple test which we can apply to tell us whether a fixed point is attractive or repellent.

If x is a fixed point:

$$\begin{aligned} |f'(x)| < 1 &\iff x \text{ is an attractor} \\ |f'(x)| > 1 &\iff x \text{ is a repeller} \end{aligned} \quad (**)$$

If the nature of the point is dependent on r then we suppose the above conditions and solve for r .

This technique to find and classify fixed points becomes cumbersome to apply multiple times and so after one or two applications we chose to proceed our investigation numerically with the following algorithm:

1. Iterate r from 0 to a maximum in large steps
2. Find the approximate values where the function bifurcates
3. For each bifurcation repeat steps 4 - 9:
4. Take $rl := r - \text{epsilon}$, $rr := r + \text{epsilon}$
5. Take the centre $rm := (rl + rr) / 2$
6. Check period at this centre rm
7. If the period at rm is less than period required set $rl := rm$
8. Otherwise set $rr := rm$
9. Stop if $|rr - rl|$ is very small

1.2 Verhulst Process

The Verhulst process takes its name from a Belgian mathematician Pierre Verhulst: he proposed a differential equation related to population dynamics in 1838 [2]. An iteratively defined exact solution to this equation takes the form:

$$x_{n+1} = x_n + rx_n(1 - x_n)$$

where x denotes a ratio between the current and maximum populations and r denotes a constant which is crucial in determining the eventual outcome of a population defined by the system. Due to the applied nature of this map we restrict r and x_0 to be real and positive.

By application of (*), there are two fixed points: $x = 0$ and $x = 1$.

By application of (**), $x = 1$ is an attractor for $0 < r < 2$ and $x = 0$ is a repeller for $r > 0$.

By application of (*), there are two 2-periodic points: $x = \frac{r + 2 \pm \sqrt{r^2 - 4}}{2r}$ for $r > 2$.

For periods greater than 2, searching for periodic points mathematically becomes too awkward and so we proceed numerically.

The algorithm defined in 1.1 returns the following results:

```
2 cycle detected at r = 2.000000
4 cycle detected at r = 2.449490
8 cycle detected at r = 2.544090
16 cycle detected at r = 2.564407
32 cycle detected at r = 2.568759
64 cycle detected at r = 2.569692
128 cycle detected at r = 2.569891
256 cycle detected at r = 2.569934
```

For $r > 2.57$, the system appears to become chaotic with no periodic points for most values of r . However, we were able to detect some cycles, showing the presence of certain non-chaotic regions. We investigate these further later in the project. The results above agree with the images in Figure 2.

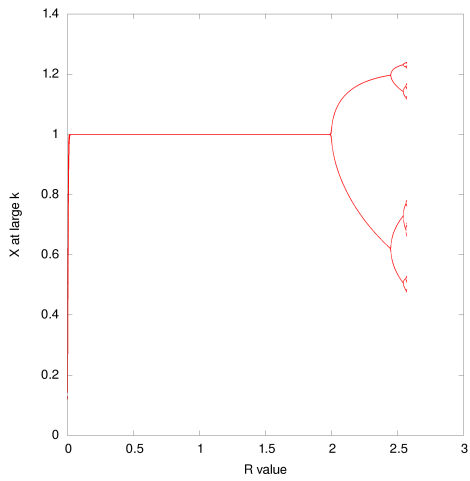


Figure 1: Verhulst process from $r = 0$ to $r = 2.57$ fixing $x_0 = 0.1$

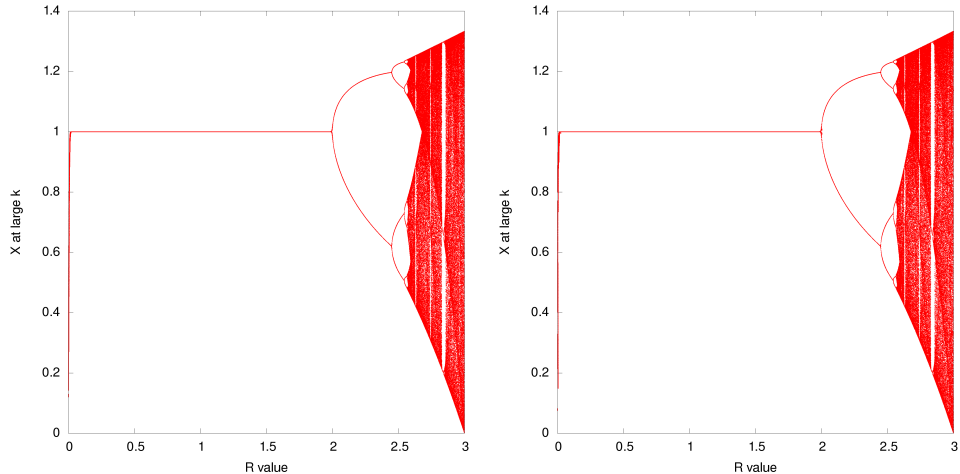


Figure 2: Verhulst process from $r = 0$ to $r = 3$ first fixing $x_0 = 0.1$ and secondly randomising in the interval $(0, 0.5)$

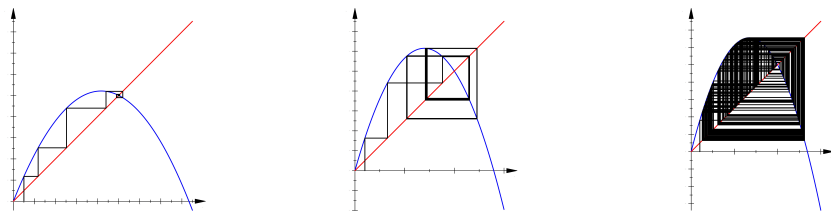


Figure 3: Verhulst Spider Diagrams for a 1-cycle, 4-cycle and chaotic system

1.3 Logistic Map

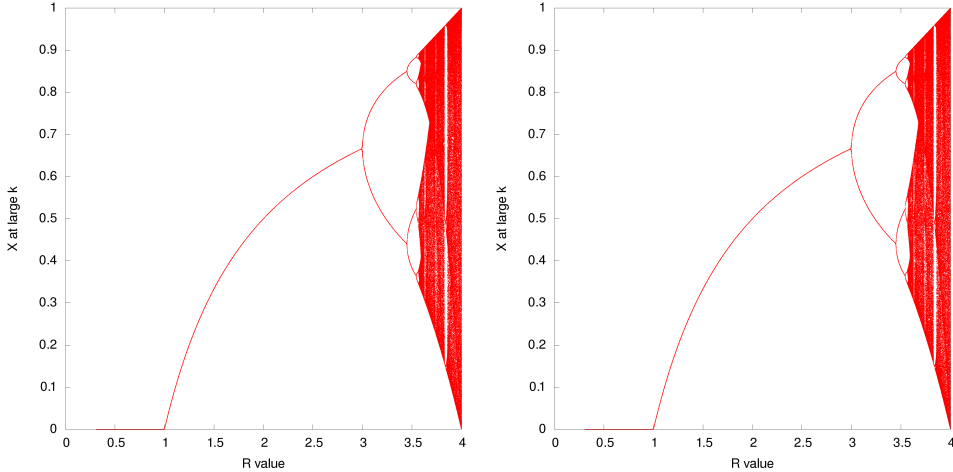


Figure 4: Logistic map from $r = 0$ to $r = 4$ first fixing $x_0 = 0.1$ and secondly randomising in the interval $(0, 0.5)$

The logistic map is similar to the Verhulst process in its application to population dynamics; it too models population growth in a discrete-time environment. Each iteration can be thought of as a new generation of individuals and as such, we again limit x_0 and r to be real and positive. The map is iteratively defined as:

$$x_{n+1} = rx_n(1 - x_n)$$

By application of (*), there are two fixed points: $x = 0$ and $x = 1 - \frac{1}{r}$.

By application of (**), $x = 0$ is an attractor for $0 \leq r < 1$ and $x = 1$ is an attractor for $1 < r < 3$.

By application of (*), there are two 2-periodic points: $x = \frac{r + 1 \pm \sqrt{r^2 - 2r - 3}}{2r}$ for $r > 3$.

As before, the polynomials reach too high a degree and so we proceed numerically.

```
2 cycle detected at r = 3.000000
4 cycle detected at r = 3.449490
8 cycle detected at r = 3.544090
16 cycle detected at r = 3.564407
32 cycle detected at r = 3.568759
64 cycle detected at r = 3.569692
128 cycle detected at r = 3.569891
256 cycle detected at r = 3.569934
```

Note that each value in the table is one more than the corresponding value for the Verhulst system. This is because the iterative function for the logistic map differs from that of the Verhulst process by the addition of a single x . This means their first derivative differs by one and so the r value for which the two fixed points act as attractors is shifted up by one; hence they satisfy the

conditions for repulsion from (**) one unit later. Higher derivatives are equal and therefore the difference in values remains the same for higher periods. For $r > 3.57$, the system appears to become chaotic with no periodic points for most values of r . However, once again, we were able to detect some cycles showing the presence of certain non-chaotic regions. This can be seen in Figure 4.

1.4 Trigonometric Map

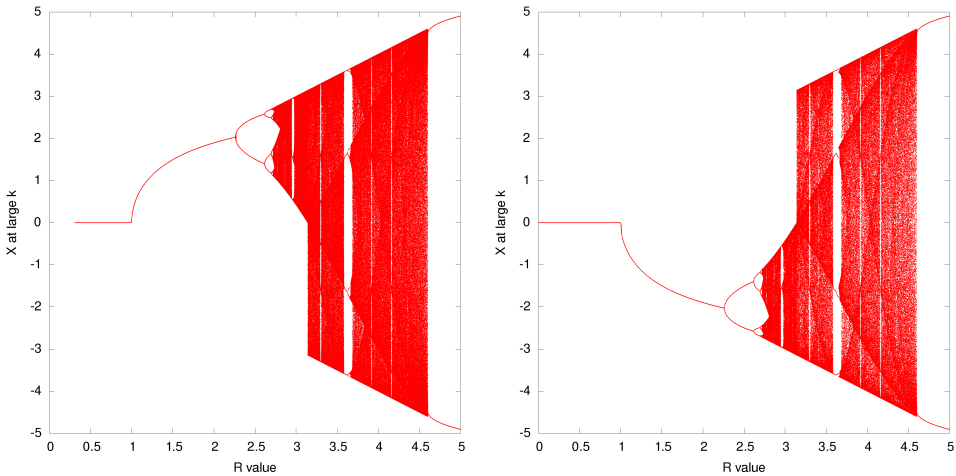


Figure 5: Trigonometric map from $r = 0$ to $r = 5$ first fixing $x_0 = 0.1$ and second fixing $x_0 = 3.15$, just above π .

The trigonometric map is analytically more sophisticated due to the introduction of the sine function. This highlights the importance of numerical methods. It is also noteworthy that this is the only map where different positive x_0 give different bifurcation diagrams: as an odd function $\sin(x)$ is perfectly reflected in the line $y = -x$, meaning that two fixed points exist equidistant from the origin. Both of these fixed points are attractors up to approximately 2.26; this means that for r below this value, any iterate which takes a negative value will remain negative under further iteration and the corresponding result holds for iterates taking positive values. This is clearly illustrated by Figure 5, where the initial value of x is positive after the first iteration and so it remains positive (after $r > \pi$ this is no longer true).
Past $r = \pi$, the bounding for the iterates is between $\pm r$ (since $r \sin(x)$ can now return a negative value with a positive input) so there is no guarantee for the sign of the next iterate.

In particular, for $\pi < x_0 < 2\pi$ the value of $\sin(x_0)$ is negative and so all resulting iterations tend towards the negative attractor. This halts at $r > \pi$ where any x_0 can tend to either the positive or negative attractors.

```

2 cycle detected at r = 1.000000
4 cycle detected at r = 2.261826
8 cycle detected at r = 2.617783
16 cycle detected at r = 2.697400
32 cycle detected at r = 2.714600
64 cycle detected at r = 2.718291
128 cycle detected at r = 2.719082
256 cycle detected at r = 2.719251
512 cycle detected at r = 2.719288

```

The results obtained above are from taking a randomised x_0 and so includes both paths before $r = \pi$. If x_0 is fixed at 0.1 then the results are identical except for an upward shift in the table, i.e. we have a 1-cycle at $r = 1.00\dots$, a 2-cycle at $r = 2.26\dots$ down to a 256-cycle at $r = 2.719\dots$

1.5 Feigenbaum Constant

The (first) Feigenbaum Constant is defined to be:

$$\lim_{n \rightarrow \infty} \frac{r_{n-1} - r_{n-2}}{r_n - r_{n-1}} \quad (1)$$

where r_n is the value of r at the n^{th} iteration. It has a value of 4.669201... which is universal to all one dimensional maps which become chaotic after a period doubling cascade [6]. We approximated the constant numerically by looking at (1) for each map. The results are:

| Map | Value |
|---------------|----------|
| Verhulst | 4.669265 |
| Logistic | 4.669294 |
| Trigonometric | 4.668826 |

Our computed values comply with the result and we achieved good approximations for relatively small number of iterations.

1.6 Final Observations

As mentioned earlier, we found certain non-chaotic regions within the chaos for each map. Upon zooming into some of these regions, we encountered bifurcation diagrams that resembled these maps. On further zooming, we found more bifurcation diagrams suggesting that the maps exhibit fractal properties. Figure 6 shows this for the Verhulst process.

Whilst perhaps initially mysterious, some enlightenment as to the presence of a period doubling cascade for all three maps can be derived from making a fairly straight-forward geometric observation.

As r increases, an attractor decays into a repeller (by (**)); this appears to lead to the existence of two focal points on either side of the square revealed by drawing equidistant lines from $y = x$ to the function f . The geometry of these points suggests that they are iterates which return to themselves with twice the period as the now decayed attractor; these points can be thought of as 2-periodic points for the function f , or fixed points for the function f^2 .

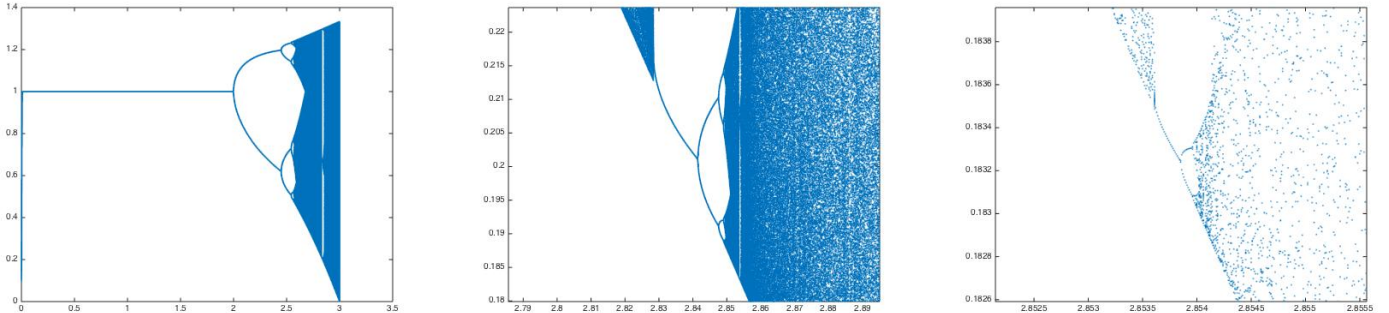


Figure 6: Verhulst Fractal Nature - Zooming in at $r = 2.84, 2.854$

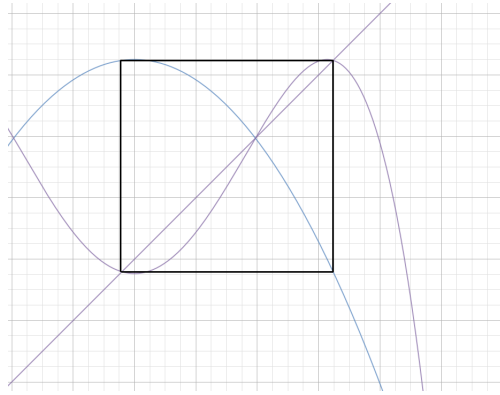


Figure 7: Showing geometrical method to find next attractor, diagram of x_{k+1} against x_k

This means that whenever an attractor decays, a pair of new attractors form either side of it at the corners of the square lying on the line $y = x$. When the fixed points of f^2 themselves decay then it is easy to see that exactly the same thing will happen (i.e. when the tangent crosses the line $y = x$ two 2-periodic points with respect to f^2 are created. The position of these attractors is again determined by drawing a square in the same manner, although the vertices will now lie on $y = x$ and on the curve defined by f^2 . We can continue this indefinitely, although the lifetime of any new attractor will decrease with each iteration as the independent variable r increases in order and so garners a greater rate of change for a given increment. Thus, the attractors decay faster and faster (which can be seen in the graphs of the cascade). No new attractors are created in any other circumstances because f^n , with n a number which is not a power of 2, will be limited to sharing fixed points with f^m , where m is the highest power of two which factorises it. As r increases it reaches a value where f becomes chaotic; at this value all f^n (for any n) begin to intersect the line $y = x$ in a seemingly random manner, causing large numbers of periodic points to form and the map to become unpredictable.

As we have demonstrated throughout, there are points within the chaotic regions

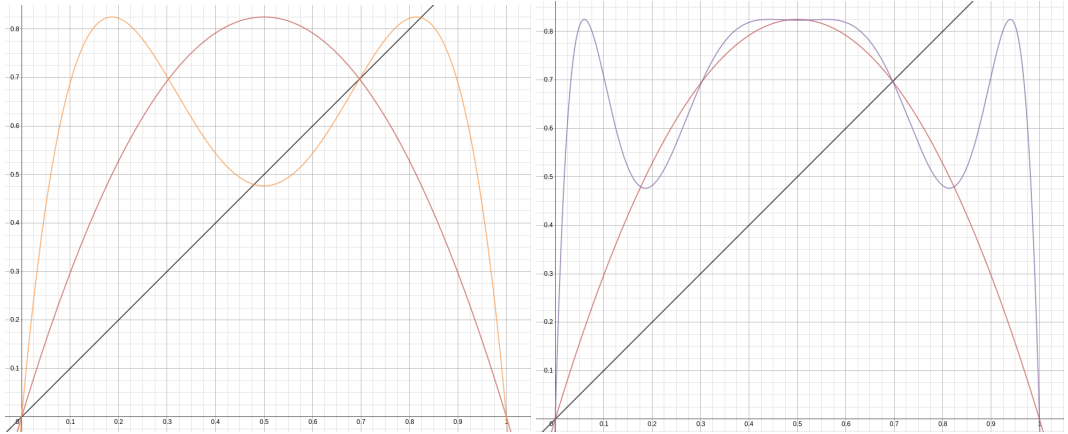


Figure 8: Left shows f and f^2 , right shows f and f^3 . The power of 3 only intersects at the same point as the power of 1

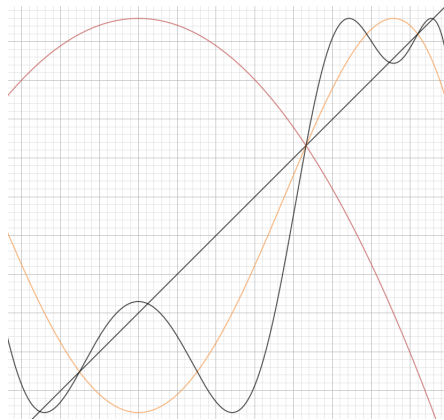


Figure 9: Further shows the bifurcation of the attractors either side of the decayed ones. Pink is f . yellow is f^2 and black is f^4 .

where it just so happens that local attractors form; they repeat the above process and thus define new bifurcations before themselves decaying back into chaos. Interestingly, the initial period of the attractors does not necessarily have to be a power of 2, however, new attractors still form in pairs around old ones, meaning that a bifurcation and period doubling cascade still occur.

2 Sets and Fractals

2.1 Definitions

The following recurrence relation takes two complex arguments z_0 and c to define an infinite sequence of complex numbers:

$$z_{k+1} = z_k^2 + c \quad (2)$$

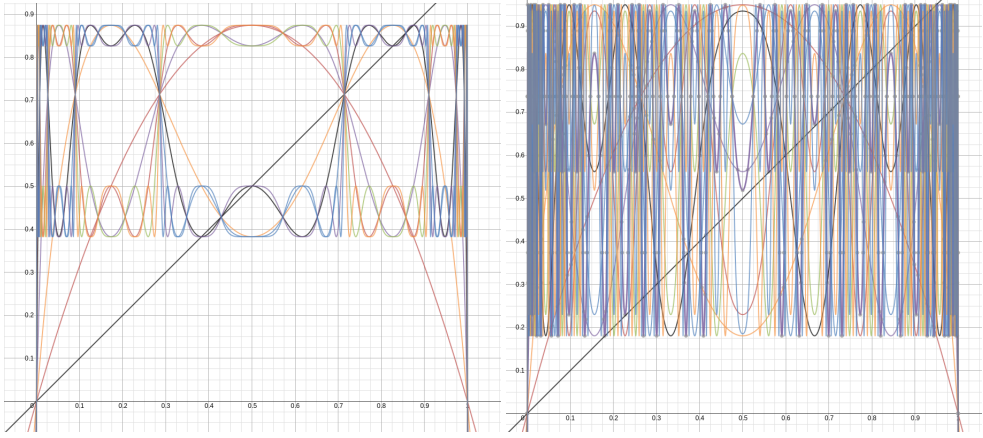


Figure 10: Showing chaos emerging as r increases

The Mandelbrot set fixes $z_0 = 0$ and is the set of all c for which the modulus of the terms of (2) remain bounded as $k \rightarrow \infty$

Julia sets do the opposite and fix c to some constant in the complex plane, varying z_0 instead. The elements are defined in the same way; as (2) is iterated, it is the set of z_0 values whose modulus remains bounded as $k \rightarrow \infty$.

The Julia and Mandelbrot sets are both orthogonal slices of the same 4-dimensional object based on equation (2). This is because (2) takes two complex arguments to generate an infinite sequence; this is the same as taking four real arguments. It can thus be thought of as an object in four dimensional space.

2.2 Mandelbrot Set

The following proof justifies the computational limit that we set on the Mandelbrot Equation. It is known as the escape criterion.

Proposition 2.1.1 $\exists k : |z_k| > 2 \iff \lim_{k \rightarrow \infty} |z_k| = \infty$
Proof: \Leftarrow

$$\begin{aligned} & \lim_{k \rightarrow \infty} |z_k| = \infty \\ & \Rightarrow \exists k : \forall n \in \mathbb{R} |z_k| > n \\ & \Rightarrow \exists k : |z_k| > 2 \\ & \Rightarrow \end{aligned}$$

Assume $\exists k : |z_k| > 2$
Fix $e > 0$ such that $z_k = 2 + e$

We know $|z_k| \geq |c|^1$

Assume $P(x) \equiv |z_{k+(x+1)}| - |z_{k+x}| \geq 2e + e^2, \quad x \in [0..m]$

We show by strong induction that $P(m+1) \equiv |z_{k+(m+2)}| - |z_{k+(m+1)}| \geq 2e + e^2$

¹ Assume that $|z_k| < |c|$. Then $|c| > |z_k| > 2$. But at $k = 1$, $|z_1| = |c| > 2$ and so wlog we begin our analysis from z_1 .

Base Case

$$\begin{aligned}|z_{k+1}| &\geq |z_k^2| - |c| = |z_k|^2 - |c| \\ \Rightarrow |z_{k+1}| &\geq (2+e)^2 - (2+e) \\ \Rightarrow |z_{k+1}| &\geq 2 + 3e + e^2 \\ \Rightarrow |z_{k+1}| - |z_k| &\geq 2 + e^2\end{aligned}$$

Inductive Step

$$\begin{aligned}|z_{k+(m+2)}| &= |z_{k+(m+1)}^2 + c| \\ \Rightarrow |z_{k+(m+2)}| &\geq |z_{k+(m+1)}^2| - |c| \\ \Rightarrow |z_{k+(m+2)}| &\geq |z_{k+(m+1)}^2| - (2+e) = |z_{k+(m+1)}|^2 - (2+e) \\ |z_{k+(m+1)}| &\geq |z_{(k+m)}| + (2e + e^2) \quad \text{from P(m)} \\ \Rightarrow |z_{(k+m)}| + 2e + e^2 &> 2 + 2e + e^2\end{aligned}$$

So $\forall x \in [0, m] P(x) \Rightarrow |z_{k+(m+1)}| > |z_{k+(m)}| > |z_{k+(m-1)}| > \dots > |z_k| > 2$

Let $A > 2e + e^2$ such that $|z_{k+(m+1)}| = 2 + A$

$$\begin{aligned}\Rightarrow |z_{k+(m+2)}| &\geq (2+A)^2 - (2+e) \\ \Rightarrow |z_{k+(m+2)}| &> 2 + 3A + A^2 \quad (\text{since } A > e) \\ \Rightarrow |z_{k+(m+2)}| - |z_{k+(m+1)}| &> 2A + A^2 > 2e + e^2\end{aligned}$$

So $\forall x \in [0, m] P(x) \Rightarrow P(m+1)$

Now choose a $d \neq 0$ such that $d \leq 2e + e^2$. We have

$$\forall n z_{k+n} \geq u_n \quad u_{n+1} - u_n = d, u_0 = 0$$

Then, by comparison with the arithmetic series u_n

$$\begin{aligned}\lim_{n \rightarrow \infty} |z_{k+n}| &= \infty \\ \Rightarrow \lim_{k \rightarrow \infty} |z_k| &= \infty\end{aligned}$$

Therefore, the mathematics allows us to exploit the condition that if for any number of iterations z_k becomes greater than 2, we can be assured that it tends to infinity and does not belong in the Mandelbrot set.

2.2.1 Plots

To visualise how the iterative function behaves on c values within the Mandelbrot set we plotted orbital diagrams. We fixed a c known to be within the set and iterated an arbitrary number of times; two resulting diagrams are shown in Figure 11. It is interesting to note that the set does not necessarily converge to a value, the only guarantee is that it does not go to infinity.

Using *Proposition 2.1.1*, we could generate an image of the Mandelbrot set as c varies in a relatively efficient manner. By creating a blank image of $n \times m$ pixels, we could map each pixel to a fixed point in the complex plane that we could then iterate upon. The algorithm would, given a point, iterate until either the

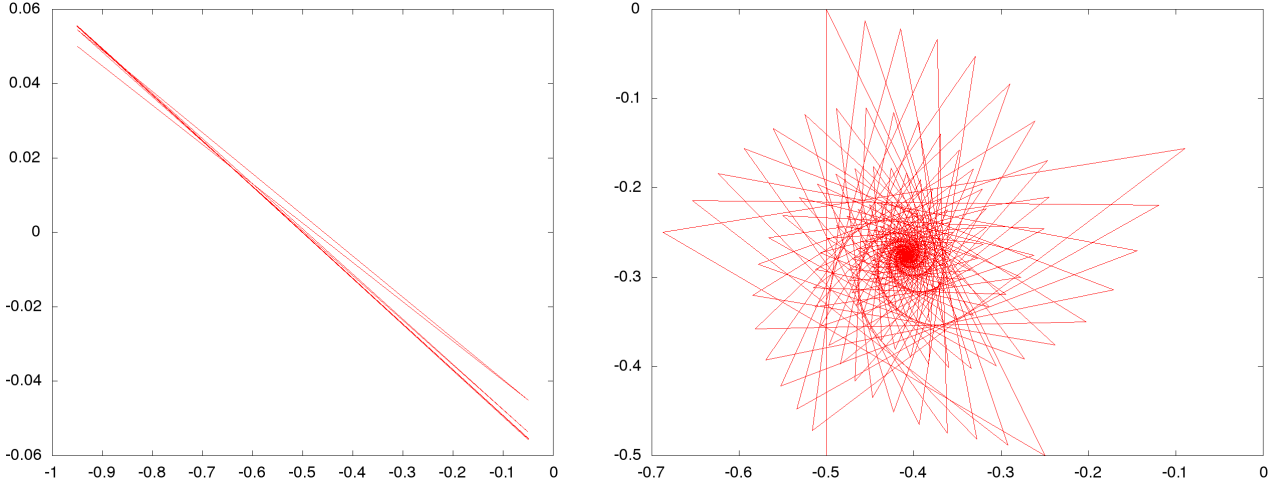


Figure 11: Plots of the mandelbrot as it converges for $c = -0.95 - 0.04i$ and $c = -0.5 - 0.5i$ respectively

absolute value was greater than two or until it timed out. We used the HSV² colour model for all of our plots, giving us the choice to plot based on hue for values we did not know the upper bound of and either saturation or colour for those we did.

Figure 12 was generated by fixing the hue and setting the points within the set black and those outside were plotted with their brightness decreased based on the iterations taken for the absolute value to pass two. The iteration number could be bounded based on the maximum iterations before it times out. At first we plotted this linearly but found that the majority of the range in brightness occurred at the boundary of the set; to create a better image we first tried storing the distribution iteration counts and plotting based on percentiles. However we found that it was more appealing to simply put the brightness to a fractional power. The final image uses the power $\frac{1}{2}$.

The next two images contained a fixed saturation and value but the hue was plotted as the iteration count modulo an arbitrary constant.

We also created images with the colour based on the distance that z_k moves as it iterates, i.e.:

$$\sum_{k=1}^{|z_k|>2} |z_k - z_{k-1}|$$

Again, this value modulo a constant is used as the hue of the pixels for the image.

In order to speed up computation, we checked the square of the absolute value against 4 instead of measuring the absolute value against two; this avoids the time consuming square root operation. Also, due to the vertical symmetry of the Mandelbrot set, for full images we only computed the top half from $0 - 1.2i$

²Hue Saturation Value: where the hue is measured from 0 - 360 and is cyclic while the saturation has a value between 0 and 1. We then mapped this directly to RGB in order to output to files.

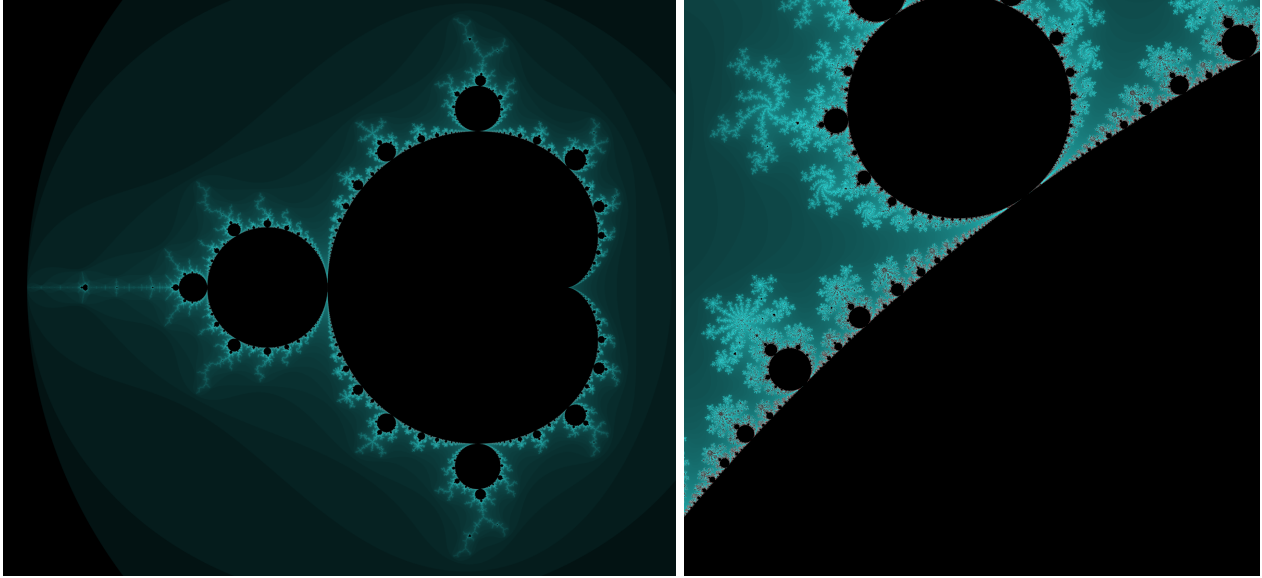


Figure 12: Mandelbrot with brightness based on iterations in full and zoomed in

which we then flipped and appended onto the base to create the final image.

Figure 13 shows the bifurcation diagram for the logistic map scaled and superimposed onto the the Mandelbrot set. Evident from observation is the fact that the period doubling cascade in the logistic map has the same ratio as the spacing between the cardioids and discs of the Mandelbrot Set. Mathematically, we can define a linear transformation from one to the other: the parameters c and r are connected by the simple equation $1 - 4c = (k - 1)^2$ [4] [5]

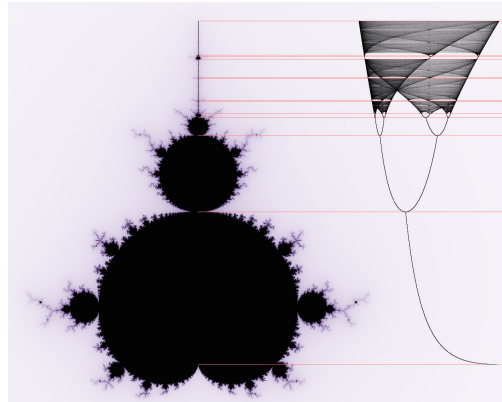


Figure 13: Verhulst overlayed onto the Mandelbrot set [4]

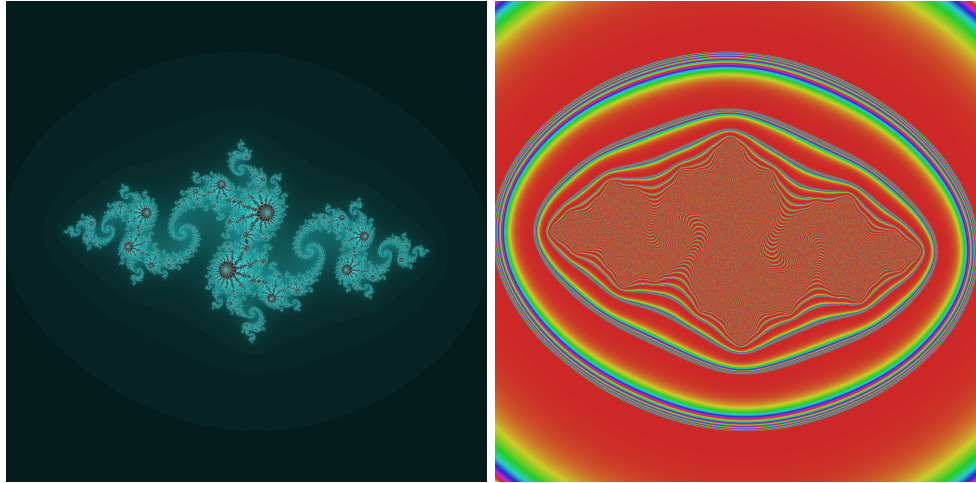


Figure 14: Julia set with $c = -0.8 + 0.156i$

2.3 Julia Sets

The Julia sets are plotted in almost exactly the same way as the Mandelbrot sets, as they use the same iterative function we can apply *Proposition 2.1.1*. In practice we fix c and map each pixel to a value of z_0 iterating until either $|z_k| > 2$ or until we reach a timeout constant. Figures 14, 15 and 16 are several Julia sets plotted both with the standard and distance based colouring schemes. The comparisons between them highlight the fractal properties and corresponding contour levels for the sets.

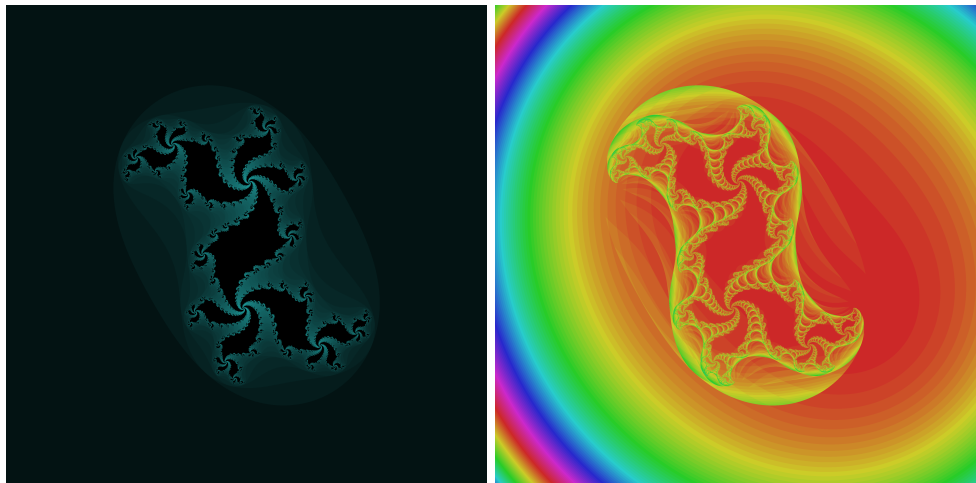


Figure 15: Julia set with $c = 0.3 + 0.5i$

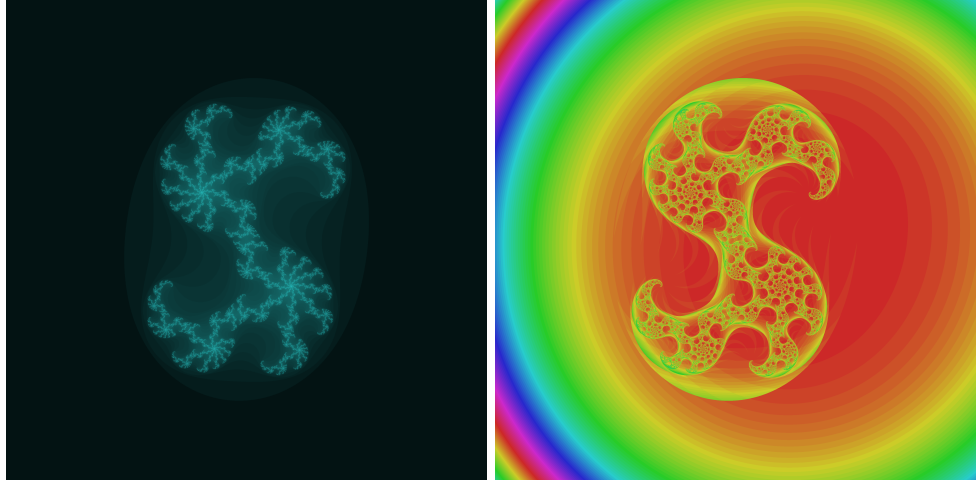


Figure 16: Julia set with $c = 3.85 - 0.1i$

2.4 Compact Sets

A set S is compact if every sequence in S has a subsequence that converges to an element contained in S , i.e.:

$$\forall (a_n) \in S \quad \exists (b_n) \leq (a_n) \quad \exists L \in S : \forall \epsilon > 0 \quad \exists N \quad \forall n \geq N \quad |b_n - L| < \epsilon$$

where we have overloaded the ' \leq ' character to mean "is a subsequence of". Both the Mandelbrot and Julia sets are compact [1] [5].

2.5 Boll's results

During Dave Boll's analysis of the Mandelbrot set, he proved that the cardioid and left disk are connected at an infinitely thin point, $c = -0.75 + 0i$. He measured the number of iterations required to escape for the point $c = -0.75 + \epsilon i$ as $\epsilon \rightarrow 0^+$. He found that the product of the number of iterations and ϵ tended to π with precision $\pm \epsilon$ [3]. We reproduced these results with ϵ as negative powers of 2; n_c refers to the minimum k such that $|z_k| > 2$.

| ϵ | $\epsilon \times n_c$ | $ \pi - (\epsilon \times n_c) $ |
|------------|-----------------------|------------------------------------|
| 2^{-0} | 3.0 | 0.14159265358979312 |
| 2^{-1} | 3.0 | 0.14159265358979312 |
| 2^{-2} | 3.25 | 0.10840734641020688 |
| 2^{-3} | 3.25 | 0.10840734641020688 |
| 2^{-4} | 3.1875 | 0.045907346410206884 |
| \vdots | \vdots | \vdots |
| 2^{-23} | 3.1415927410125732 | $8.742278012618954 \times 10^{-8}$ |
| 2^{-24} | 3.1415927410125732 | $8.742278012618954 \times 10^{-8}$ |

Boll carried out a similar investigation into the pole of the main cardioid by calculating the number of iterations for $c = 0.25 + \epsilon + 0i$ as $\epsilon \rightarrow 0^+$. This time

$\sqrt{\epsilon} \times n_c$ tends to π which we have again reproduced with powers of 2.

| ϵ | $\sqrt{\epsilon} \times n_c$ | $ \pi - (\sqrt{\epsilon} \times n_c) $ |
|------------|------------------------------|----------------------------------------|
| 2^0 | 2.0 | 1.1415926535897931 |
| 2^{-1} | 2.121320343559643 | 1.0202723100301503 |
| 2^{-2} | 2.5 | 0.6415926535897931 |
| 2^{-3} | 2.4748737341529163 | 0.6667189194368768 |
| 2^{-4} | 2.75 | 0.3915926535897931 |
| \vdots | \vdots | \vdots |
| 2^{-52} | 3.218175321817398 | 0.07658266822760496 |
| 2^{-53} | 3.1822518672868894 | 0.04065921369709624 |

The reasons for π emerging seemingly from nowhere is illuminated by the solutions of the difference equations defining the Mandelbrot set[3]. The analytical solutions are, unfortunately, beyond the scope of this project.

References

- [1] Jonathon Fraser. An introduction to julia sets. Available from http://www.gvp.cz/~vinkle/mafynet/GeoGebra/matematika/fraktaly/linearni_system/julia.pdf. Accessed: 2015-03-19.
- [2] Edmund Robertson John O'Connor. Mactutor archive. Accessible from <http://www-history.mcs.st-andrews.ac.uk/Mathematicians/Verhulst.html>.
- [3] Aaron Klebanoff. π in the mandelbrot set. Available from www.worldscientific.com/doi/pdfplus/10.1142/S0218348X01000828. Accessed: 2015-03-16.
- [4] Georg-Johann Lay. Verhulst overlayed on mandelbrot set. Available from <http://upload.wikimedia.org/wikipedia/commons/b/b4/Verhulst-Mandelbrot-Bifurcation.jpg>. Accessed: 2015-03-16.
- [5] Benoit Mandelbrot Michael Frame and Nial Neger. Fractal geometry. Available from <http://classes.yale.edu/fractals/>. Accessed: 2015-03-15.
- [6] Eric W. Weisstein. *Concise Encyclopedia of Mathematics*. CRC, 2003. Accessed: 2015-03-19.